Low temperature magnetoresistive effects and coulomb blockade in La$_{0.7}$Ca$_{0.3}$MnO$_3$ nanoparticles synthesis by auto-Ignition method

Aamir Minhas Khan[1], Arif Mumtaz[2], Syed Khurshid Hasanain[2], Anwar Ul Haq[1]

[1]Department of Physics, Air University, Islamabad, Pakistan; aamir.minhas@mail.au.edu.pk
[2]Department of Physics, Quaid-I-Azam University, Islamabad, Pakistan; minhas.qau@gmail.com

ABSTRACT

Electrical transport properties of the La$_{0.7}$Ca$_{0.3}$MnO$_3$ nanoparticles have been investigated in the temperature range 300 to 9 K as a function of magnetic field. Samples were prepared by auto-ignition method. In low temperature regime from 40 to 9 K, an increase in the resistivity has been observed. This effect is found to decrease as magnetic field is increased. It is assumed that these effects are due to the magnetic contacts between the nanoparticles.

Keywords: CMR (Colossal Magnetoresistance) CB (Coulomb Blockade)

1. INTRODUCTION

Magnetoresistance (MR) phenomenon, in which the electrical transport properties are strongly affected by applied magnetic fields, was first reported in 1988 [1] in metallic multilayers. Similar results were followed by granular metallic systems [2,3] and in permalloy/Al$_2$O$_3$/CoFe junctions [4]. All of these records show that new tools are now reachable to obtain artificial MR by manipulating the micro/nanostructure of metallic compounds. Thus Magnetic nanoparticles exhibit interesting electronic and magnetic properties arising due to the structural and magnetic disorders in their surfaces especially in nano-sized perovskites [5,6]. In early 1990s, in mixed-valence manganese oxides (hereafter referred to as *manganites*) a new kind of MR was rediscovered [7]. Under a field of several Tesla it was possible to achieve MR at temperatures relatively close to transition temperature, leading to the name of colossal MR (CMR). This class of oxides was theoretically modeled in 1950s [8,9], when the first studies were carried out on the crystallographic structure, and found to have "perovskite "structure. *CMR* properties of these materials make them

technologically important for applications in magnetore-sistive devices [5,10], principally in magnetic recording or magnetic data storage devices. Intrinsic phase separation in (CMR) material is also an important phenomenon leading to the new applications of spintronics [11,12] Within the past decade, one-dimensional nanowires and nanowire arrays have captured the interests of many groups in a wide variety of fields, mainly due to their unusual properties and potential for integration into and miniaturization of current technologies.

Therefore, hole-doped manganese perovskites L$_{1-x}$A$_x$MnO$_3$, where L and A are trivalent lanthanide and divalent alkaline earth ions respectively, have been studied extensively [13,14]. By changing values of x in La$_{1-x}$Ca$_x$MnO$_3$ we may get a variety of magnetic and transport states in the material, ranging from different antiferromagnetic insulators to ferromagnetic metals. Here we focus on x = 3, because it lies in ferromagnetic /metallic phase in the phase diagram [15].

The resistivity of the nano sized manganite below 50 K under zero magnetic field is reported by many workers. D. Niebieskikwiat [16] synthesized magnatites by three different methods namely Gel Combustion (GC), Urea Sol-Gel (USG) and Liquid Mix (LM). The particle size in the samples was 30 nm and ρ of the samples follow the order $\rho_{GC} > \rho_{USG} > \rho_{LM}$. The low temperature increase of ρ was not observed in sample of 95 nm particle size. MA L´opez-Quintela [17] also observed the maximum upturn in very low temperature for 60 nm as compared to 500 nm. Y. G. Zhao [18] observed the same trend in thin film, *i.e.* maximum upturn for 36 nm as compared to 108 nm. M. García-Hernández [6,19] also observed the maximum upturn for 20 nm as compared to 80 nm. In all of these papers explanation is followed by $T^{-1/2}$ curve fitting. The $T^{-1/2}$ model accounts for the low-temperature resistance of granular metals embedded within an insulating matrix, and it is only valid in the tunneling regime, where typical intergrain resistances are

much larger than $h/e^2 \sim 12 \times 10^3$ Ω. It also assumes that the energy barriers are inversely proportional to the grain radius. M. García-Hernández [6,19] also observed the effect of very high magnetic field of 9 T on the low temperature upturn and explained on the basis of reformulation of the $T^{-1/2}$ model.

2. EXPERIMENTAL PROCEDURES

Nanoparticles of $La_{0.7}Ca_{0.3}MnO_3$ were synthesized by citrate auto-ignition method [20]. La_2O_3, $CaCO_3$, $Mn(CH_3COO)_2 \cdot 4H_2O$ and $C_6H_8O_7$ were used in stochiometric amounts as starting materials. First La_2O_3 and $CaCO_3$ were dissolved into HNO_3 to convert them into their corresponding water soluble nitrates. $Mn(CH_3COO)_2 \cdot 4H_2O$ and citric acid were dissolved in water separately. All the solutions were mixed and stirred for 4 - 5 minutes to make a homogeneous solution and then citric acid was added to it as a chelating agent. To avoid precipitation, pH value of the solution was adjusted to a neutral value of 7 using the aqueous NH_3 solution. That solution was slowly evaporated at 80˚C - 90˚C for 60 to 90 minutes, which resulted brown colored viscous gel. This was further heated in a box furnace at ~250˚C. After about 30 minutes, the gel was foamed; swelled and large volume of gases was evolved leading to an automatic ignition with glowing flints. This produced highly porous black fluffy material with fine powder of about 20 nm (called a precursor). The precursor was annealed at 1000˚C for 10 hours. Before pelletization, structure of the powder was studied using powder X-ray diffraction (*XRD*). **Figure 1** shows the XRD pattern. All peaks could be indexed for an orthorhombic unit cell of a = 5.4412 Å b = 7.6637 Å c = 5.4479 Å. The phase defection limit of XRD is 5%. If it is less than 5% then, no XRD peak will be defected. As we assume that our sample has, if at all, less than 5% such phase. The average particle size as estimated by Scherrer's formula was 40 nm.

For the resistivity measurements rectangular pellet of the samples (length = 4.7 mm, width = 3.4 mm, thickness = 1.6 mm) were prepared. Powdered sample was first mixed with few drops of liquid binder Poly Vinyl Alcohol (PVA), compressed under pressure of 7 - 8 ton and then heated at 650˚C for 5 hours to get good compact discs. The four probe configuration was used to measure resistivity values. For the resistivity $\rho(T)$ measurement under magnetic field, a Hall probe was used in which, D.C magnetic field was applied perpendicular to the flow of current.

3. RESULTS AND DISCUSSION

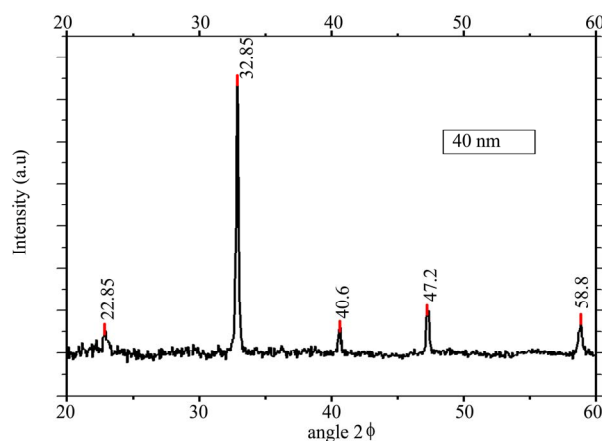The electrical transport property constitutes the most

Figure 1. Evolution of the XRD patterns.

attractive physical property of the manganites due to their high *CMR* values [17]. **Figure 2(a)** shows the resistivity of the sample as a function of temperature and magnetic field (H = 200 Oe, H = 1 kOe and H= 4 kOe).

Resistivity without magnetic field, increases with the decrease of temperature and exhibits a pronounced peak at metal-insulator transition $T_{MI} \approx 256$ K due to paramagnetic to ferromagnetic transition [21]. The susceptibility measurements also show a peak in $d\chi'/dT$ versus temperature curve conforming paramagnetic ferromagnetic transition at 256 K, as shown in **Figures 2(b) and 3** and their trend is shown in **Figure 4**. Resistivity between temperature range of 300 K to 256 K shows negative temperature coefficient of resistivity (*i.e.*, $d\rho/dT < 0$) indicating an insulating nature. Whereas the positive temperature coefficient (*i.e.*, $d\rho/dT > 0$) between 256 K to 40 K, *i.e.*, below T_{MI} displays a metallic behavior of the sample, together with a paramagnetic to ferromagnetic transition in the close vicinity [22].
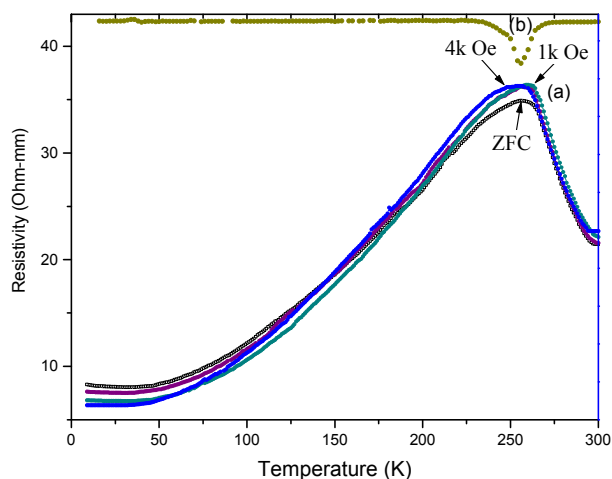

Figure 2. (a) Resistivity versus temperature curves under different magnetic field. (b) Susceptibity derivative versus temperature curve.
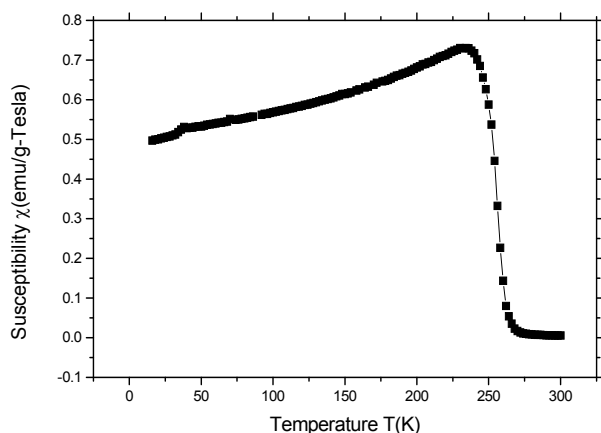
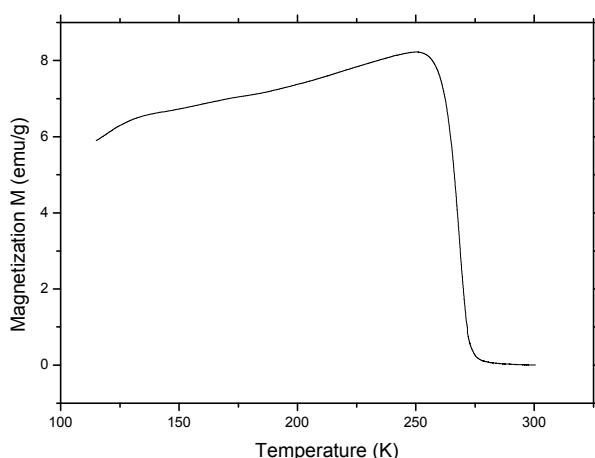**Figure 3.** Susceptibility versus Temperature plot.

Figure 4. Magnetization versus Temperature Plot.

In the temperature range $T < 40$ K, resistivity values without magnetic field exhibits a minima in $\rho(T)$ and an increase in resistivity values observed below 35 K. Here $d\rho/dT$ values again indicate a negative slope leading to an insulating behavior in ferromagnetic phase. In the temperature range from 35 K to 9 K, the increase in resistivity values is of the order of 8.049 ohm-mm to 8.829 ohm-mm, and $d\rho/dT$ is −0.0236 (ohm-mm/K) at 9 K. This effect has not been reported in high-quality single crystals [17]. Since our material is polycrystalline and consists of nanoparticles as such it may due to an electrostatic blockade of carriers between grains [17] and will be discussed later on in detail.

It is interesting to note that T_{MI} values are changing due to application of magnetic field but no field dependence is observed. Values of T_{M-I} are 256 K, 259 K and 258 K for the magnetic fields of 200 Oe, 1 kOe and 4 kOe field respectively. However, $d\rho/dT$ is negative in the temperature range of 300 K to 256 K and is positive below T_{M-I} up to 40 K, showing no significant difference as compare to zero field values. It is worth mentioning

that the values of the resistivity at T_{M-I} are independent of the magnetic field and are 34.911 ohm-mm, 36.227 ohm- mm, 36.382 ohm-mm and 36.271 ohm-mm for magnetic fields of zero, 200 Oe, 1 kOe and 4 kOe, respectively as shown in **Table 1**. Room temperature normalized resistivities are also field independent (**Figure 5**). This is in contradiction to the work of P K Siwach, M. Garcı´a- Herna´ndez, Ning Zhang and B. Roy [6,15,22,23], where resistivity at T_{M-I} decreases with the increase of magnetic field, further investigation is in hand to explain the reasons. Value of the $d\rho/dT$ at 9 K increases with the increase of the magnetic field, and is of the order of −0.012 ohm-mm/K, −0.007 ohm-mm/K and 0 ohm-mm/ K for the magnetic fields of 200 Oe, 1 kOe and 4 kOe magnetic field respectively. Also below 35 K the increase of resistivity is 0.244 ohm-mm, 0.11 ohm-mm, 0.086 ohm-mm and 0 ohm-mm at zero, 200Oe, 1kOe and 4kOe, respectively as shown in **Table 1**. This variation in the $d\rho/dT$ is also reported in thin films of manganite [6,19] which was more prominent in the smaller grain sized particles [17]. But to best of our knowledge this zero slope behavior of the resistivity has not been reported earlier in polycrystalline nanoparticles.

To understand the low temperature resistivity $\rho(T)$ behavior of the nanoparticles, we may use core-shell model as proposed by Zhang *et al.* [22]. This model assumes that the core of nanoparticles has the properties of the bulk material and low freezing temperature for spins in the outer surface layer of the particles [22]. We may analyze the resistivity curves as the sum of these two contributions, *i.e.*,

$$\rho(T) = A\rho_0 + B\exp(D/T)^{1/2}$$

where, ρ_0 stands for the resistivity of the bulk material without increase in resistivity below 40 K. The second term describes the Coulomb Blockade CB effect, *i.e.*
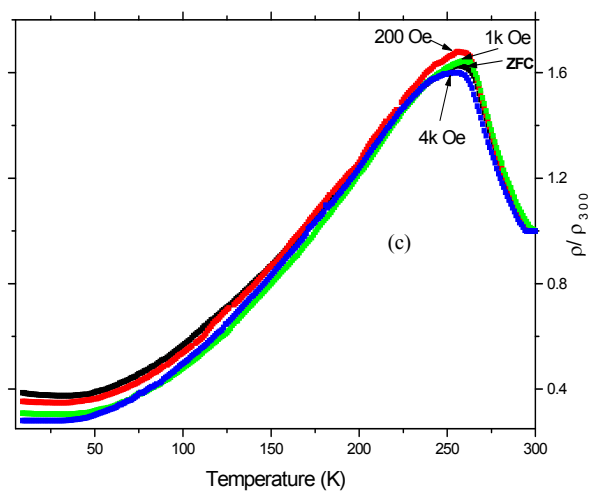

Figure 5. Room temperature normalized resistivity.

Table 1. Effects of magnetic field on resistivity parameters.

| Magnetic Field (k Oe)	T_{MI} (K)	Resistivity ρ at T_{MI} (ohm-mm)	Increase of resistivity ρ (ohm-mm). (below 35 K)	$d\rho/dT$ at 9 K (ohm-mm/K)	Slope D calculated from **Eq.1**.
Zero	256	34.911	0.82	−0.023	0.095
0.2	256	36.227	0.1109	−0.012	0.047
1	259	36.382	0.0867	−0.007	0.032
4	258	36.271	0	0	0

increase in resistivity below 40 K [6,19]. Where A and B are constants.

$$\rho(T) \, \alpha \, \exp(D/T)^{1/2} \qquad (1)$$

The plot of log ρ vs T shows a best fit for log ρ vs $T^{-1/2}$ instead of the T^{-1} postulated for a pure CB effect [19]. $T^{-1/2}$ model assumes the charging energy E_C to be particle size dependent [6,24]. The slopes of the lines (D) shown in **Figure 6**, are proportional to the electrostatic charging energy E_C [25,26] and are magnetic field dependent also **Figure 7** shows the magnifying slopes. This variation in charging energies E_C with the applied magnetic field may not be explained by a standard CB [6] model.

This effect may be explained if we take into account the transportation of electrons from one Mn site to the other by double exchange DE. The basic idea of double exchange is that the initial and final states are degenerate states, leading to a delocalization of the hole on the Mn^{4+} site or electron on the Mn^{3+} site. Thus the transfer of an electron occurs simultaneously from Mn^{3+} to O^{2-} and from O^{2-} to Mn^{4+}; this process is a real charge transfer process and involves an overlap integral between Mn 3d and O 2p orbitals [27]. In 1955 Anderson and Hasegawa introduced modified model, in which they treat spin magnetic moments of each Mn ion classically and the mobile electron quantum mechanically. They showed that electron transfer probability t_{eff} between neighboring Mn ions depends on the angle θ between their magnetic moments as $t_{eff} = t \cos(\theta/2)$. Which varies from 1 for $\theta = 0$ to zero for $\theta = 180°$ [28] (i-e transfer of electron between neighboring Mn ions is favored when angle between their spin magnetic moments is zero and this transfer become more difficult when orthognality increases).

Large number of dangling bonds or existence of the noncoordination atoms in the surfaces, structure sensitivity of the material and defects all together effect the double-exchange DE interaction in the surface. The insulating property exhibited by the ρ(T) curve, below 35 K in the ferromagnetic phase, may be due to the breakdown of the DE mechanism caused by the broken Mn–O–Mn bonds at the surface of the nanoparticles and the translational symmetry breaking of the lattice [23]. Taking into account the structure sensitivity of the magnetic configuration of such material [22] we can suppose that with the applied magnetic field spin magnetic mo-
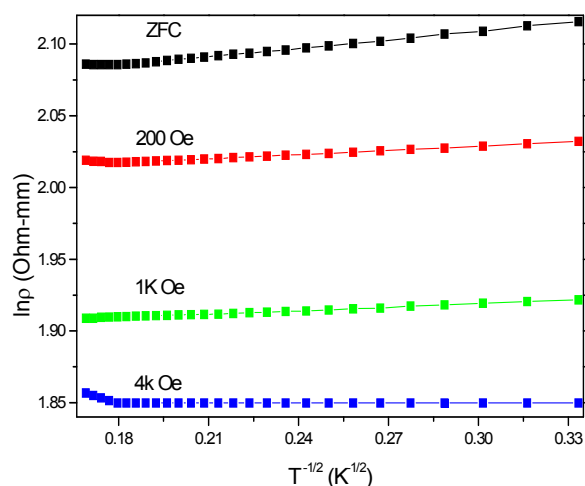
Figure 6. Natural Log of Resistivity as a function of $T^{-1/2}$.
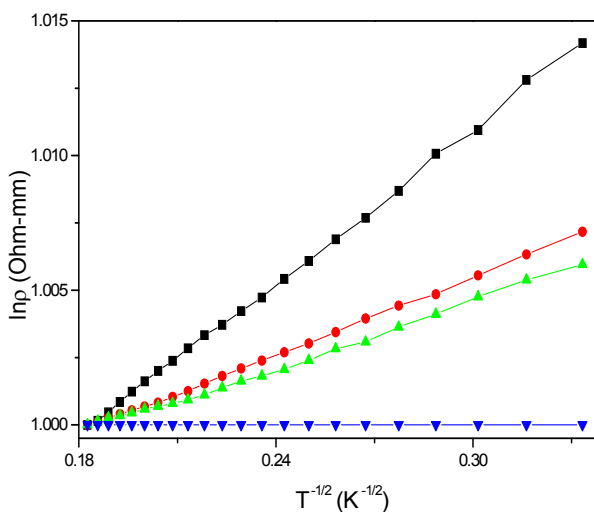
Figure 7. Magnifying slope of the curve immerging from the same point.

ments of two neighboring Mn ions, through O ion between them, at the neighboring nanoparticles get aligned [6,19]. Which may give rise to the establishment of a good magnetic contact between the neighboring nanoparticles as suggested by M. Garcı́a-Herná ndez [6]? This provides new productive conduction channels for the electrons across the particle boundaries as claimed in the literature [29]. These magnetic contacts help carriers to flow from particle to particle. If N is number of channels at the contact then conductance must be of the order

of Ne^2/h [6]. Furthermore, the capacitances of individual particles are renormalized by coupling to the other particles and, therefore, are no longer determined solely by the particle radius as suggested $E_C = e^2/4\pi\varepsilon_0\varepsilon d$. The following hypothesis makes the main difference with respect to the standard *CB* model.

Particle capacitances mainly depend on the quality of the contacts established with the neighboring particles and therefore on the connectivity of the system and particles with good contacts show no CB effects, even if their radii are small [6], as shown in the **Figure 8** for resistivity at 4 kOe (*i.e.* there is no rise in temperature below 0 K for 4 K Oe magnetic field). In this context, connectivity may also be understood in a broad sense. Realizations of such magnetic contacts microscopic weak links are misaligned Mn spins at the surface [29-32], distortions of the Mn-O-Mn angles due to structurally unbalanced environments at the grain surface and impurities or defects [6]. The blocked spins in the surface can be aligned by external magnetic field, just like in crystals [6]. The average relative angle of the local spins, in surface Δf_s is larger than that in body phase Δf_b at a given temperature below T_C, *i.e.* $\Delta f_s > \Delta f_b$ when $T < T_C$. Two neighboring nanoparticles can be electrically connected only when atoms of both sides, on the edge of nanoparticle, overlap each other partly and form a Mn-O-Mn. This demands small enough interparticles distance *i.e.* half the Mn-O-Mn bond length [22], which might be achieved by pallet preparation of the sample under high enough pressure (*i.e.* under 7 ton) and heating (heating at 650°C for 5 hours). Also a Mn ion and an O^{-2} ion, respectively, sit at the two sides of a connective point of neighboring nanoparticles. As the field increases blocked Mn spins at the surface of a nanoparticle get align and probability of such a DE phenomenon at the surface increases, which depends upon
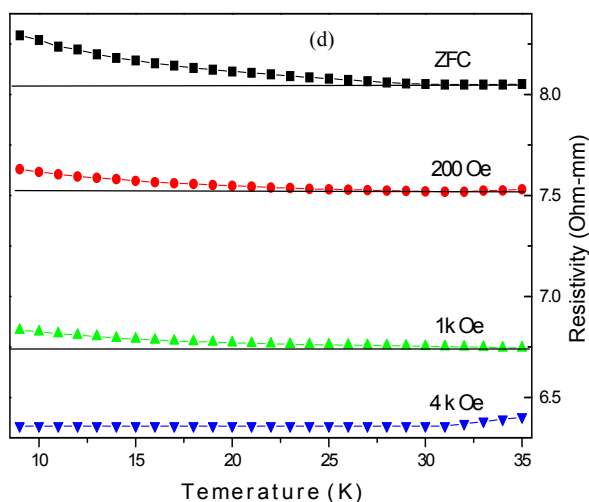
the surface spin population [22]. Magnetic field stabilizes the contact points which tend to strengthen coupling of the nanoparticles. Thus in this way coupling between neighboring nanoparticles enhances with the application of magnetic field, leading to delocalization of the charges to neighboring particles. As a result, a decrease of the resistivity is observed experimentally, upon application of a magnetic field below 35 K.

4. CONCLUSIONS

Nanoparticles of $La_{0.7}Ca_{0.3}MnO_3$ have been synthesized by citrate auto-ignition method and their electrical properties (resistivity) investigated. Below 35 K, increase in the resistivity values with the decrease in temperature is observed without magnetic field. Below 35 K charging energy was found to be sensitive to the application of a magnetic field, which could not be explained by the pure *CB* model. Charging effect dependence upon magnetic field was explained assuming that there exist good contacts between the neighboring nanoparticles due to alignment of the magnetic Mn spins at the surfaces of the neighboring nanoparticles with the magnetic field. These contacts delocalize the charges to neighboring nanoparticles.

Figure 8. Resistivity curves below 35 K.

REFERENCES

[1] Baibich, M.N., Broto, J.M., Fert, A., Nguyen, Van Dau, F., Petroff, F., Etienne, P., Creuzet, G., Friederich, A. and Chazelas, J. (1988) Giant magnetoresistance on (001)Fe/(001) Crmagnetic superlattices. *Physical Review Letters*, **61**, 2472-2475. doi:10.1103/PhysRevLett.61.2472

[2] Berkowitz, A.E., Mitchell, J.R., Carey, M.J., Young, A.P., Zhang, S., Spada, F.E., Parker, F.T., Hutten, A. and Thomas, G. (1992) Giant magnetoresistance in heterogeneous Cu–Co alloys. *Physical Review Letters*, **68**, 3745-3748. doi:10.1103/PhysRevLett.68.3745

[3] Xiao, J.Q., Jiang, J.S. and Chien, C.L. (1992) Giant magnetoresistance in nonmultilayermagnetic systems. *Physical Review Letters*, **68**, 3749-3752. doi:10.1103/PhysRevLett.68.3749

[4] Moodera, J.S., Kinder, L.S., Wong, T.M. and Meservey, R. (1995) Large magnetoresistance at room temperature in ferromagnetic thin films tunnel junctions. *Physical Review Letters*, **74**, 3273-3276. doi:10.1103/PhysRevLett.74.3273

[5] McComick, P.G. and Street, R. (2003) Surface spin disorder and exchange bais in $La_{0.7}Ca_{0.3}MnO_3$ nanoparticles synthesised by mechanochemical prossesing. *Reviews on Advanced Materials Science*, **5**, 76-81.

[6] Garcı́a-Hernández, M., Guinea, F., de Andrés, A., Martı́nez, J.L., Prieto, C. and Vázquez, L. (2000) Coulomb blockade versus intergrain resistance in colossal magnetoresistive manganite granular film. *Physical Review B*, **61**, 9549-9552.

[7] von Helmolt, R., Wecker, J., Holzapfel, B., Schultz, L. and Samwer, K. (1993) Giant negative magnetoresistance

in perovskitelike La2/3Ba1/3MnOx ferromagnetic films. *Physical Review Letters*, **71**, 2331-2334. doi:10.1103/PhysRevLett.71.2331

[8] Jonker, G.H. and Van Santen, J.H. (1950) Ferromagnetic compounds of manganese with perovskite structure. *Physica*, **16**, 337-345. doi:10.1016/0031-8914(50)90033-4

[9] Wollan, E.O. and Koehler, W.C. (1955) Neutron diffraction studies of the magnetic properties of the series of perovskite-type compounds [(1 − x)La, xCa]MnO$_3$. *Physical Review*, **100**, 545-563. doi:10.1103/PhysRev.100.545

[10] Shankara, K.S., Kara, S., Subbannab, G.N. and Raychaudhuria A.K. (2004) Enhanced ferromagnetic transition temperature in nanocrystalline lanthanum calcium manganese oxide (La$_{0.67}$Ca$_{0.33}$MnO$_3$). S*olid State Communications*, **129**, 479-483.

[11] Lu, Y. *et al.* (1996) *Physical Review B*, **54**, R8357.

[12] Sun, J.Z. *et al.* (1997) Temperature dependent, non-ohmic magnetoresistance in doped perovskite manganate trilayer junctions. *Applied Physics Letters*, **70**, 1769.

[13] Rao, C.N.R. and Raveau, R. (1998) Colossal magnetoresistance, charge ordering and related properties of manganese oxides. 1st Edition, World Scientific Publishing Co. Pte. Ltd, Singapore.

[14] Chahara, K., Ohno, T., Kasai, M. and Kozono, Y. (1993) Magnetoresistance in magnetic manganese oxide with intrinsic antiferromagnetic spin structure. *Applied Physics Letters*, **63**, 1990. doi:10.1063/1.110624

[15] Siwach, P.K., Singh, H.K. and Srivastava, O.N. (2008) Low field magnetotransport in manganites. *Journal of Physics Condensed Matter*, **20**, 1-43. doi:10.1088/0953-8984/20/27/273201

[16] Niebieskikwiat, D., Sa´nchez, R.D., Lamas, D.G. and Caneiro, A. (2003) Tunneling barrier in nanoparticle junctions of La$_{2/3}$(Ca,Sr)$_{1/3}$MnO$_3$: Nonlinear current—voltage characteristics. *Journal of Applied Physics*, **93**, 6305-6310. doi:10.1063/1.1568156

[17] Lopez-Quintela, M.A., Hueso, L.E., Rivas, J. and Rivadulla F., (2003) Intergranular magnetoresistance in nanomanganites. *Nanotechnology*, **14**, 212-219. doi:10.1088/0957-4484/14/2/322

[18] Zhao, Y.G. (2005) Electrical transport and magnetic properties of nanostructured La$_{0.67}$Ca$_{0.33}$MnO$_3$. *Applied Physics A*, **81**, 607-610.

[19] Garcia-Hemandez, M., de Andres, A., Martinez, J.L., Prieto, C., Munoz. A., Vazquez, L. and Superfi, Y. (1999) Intergranular coulomb blockade in thin films of magnetoresistive manganites. *Vacio*, **9**, 44-47. http://redalyc.uaemex.mx/redalyc/pdf/942/94200911.pdf

[20] Krishnamoorthy, C., Sethupathi, K. and Sankaranarayanan, V. (2004) Synthesis, Characterisation and Electrical Transport Properties of Manganite Nanoparticles. *International Symposium of Research Students on Material Science and Engineering*, 20-22 December 2004, Chennai, India. http://metallurgy.iitm.ac.in/isrs/isrs04/cd/content/Papers/NM/PO-NM-8.pdf

[21] Mahesh, R., Mahendiran, R., Raychaudhuri, A.K. and Raom, C.N.R. (1996) Effect of particle size on the giant magnetoresistance of La$_{0.7}$Ca$_{0.3}$MnO$_3$. *Applied Physics Letters*, **68**, 2291-2293. doi:10.1063/1.116167

[22] Zhang, N., Ding, W., Zhong, W., Xing, D. and Du, Y. (1997) Tunnel-type giant magnetoresistance in the granular perovskite La$_{0.85}$Sr$_{0.15}$MnO$_3$. *Physical Review B*, **56**, 8138-8142.

[23] Roy, B., Poddar, A. and Das, S. (2006) Electrical transport properties and magnetic cluster glass behavior of Nd$_{0.7}$Sr$_{0.3}$MnO$_3$ nanoparticles. *Journal of Applied Physics*, **100**, 104318.

[24] Mitani, S., Takahashi, S., Takanashi, K., Yakushiji, K., Maekawa, S. and Fujimori, H. (1998) Enhanced magnetoresistance in insulating granular systems: evidence for higher-order tunneling. *Physical Review Letters*, **81**, 2799-2802. doi:10.1103/PhysRevLett.81.2799

[25] Sheng, P., Abeles, B. and Arie, Y. (1973) Hopping Conductivity in Granular Metals. *Physical Review Letters*, **31**, 44-47. doi:10.1103/PhysRevLett.31.44

[26] Balcells, L., Martinez, B., Sandiumenge, F. and Fontcuberta, J. (2000) Low-temperature magnetotransport in nanometric half-metallic ferromagnetic perovskites. *Journal of Physics*: *Condensed Matter*, **12**, 3013-3018. doi:10.1088/0953-8984/12/13/311

[27] Zener, C. (1951) Interaction between the d-shells in the transition metals: II. Ferromagnetic compounds of manganese with perovskite structure. *Physical Review*, **82**, 403-405. doi:10.1103/PhysRev.82.403

[28] Anderson, P.W. and Hasegawa, H. (1955) Considerations on Double Exchange. *Physical Review*, **100**, 675-681.

[29] de Andres, A., Garcia-Hernandez, J.L.M. and Prieto, C. (1999) Low-temperature magnetoresistance in polycrystalline manganites: Connectivity versus grain size. *Applied Physics Letters*, **74**, 3884-3887.

[30] Guinea, F. (1998) Spin-flip scattering in magnetic junctions. *Physical Review B*, **58**, 9212.

[31] Caldero´n, M. J., Brey, L. and Guinea, F. (1999) Surface electronic structure and magnetic properties of doped manganites. *Physical Review B*, 60, 6698-6704. doi:10.1103/PhysRevB.60.6698

[32] Ott, F., Barberan, S., Lunney, J. G., Coey, J. M. D., Berthet, P., de Leon-Guevara, A.M. and Revcolevschi, A. (1998) Quantized conductance in a contact between metallic oxide crystals. *Physical Review B*, **58**, 4656. doi:10.1103/PhysRevB.58.4656